Sensors and Actuators B 198 (2014) 285–293

Contents lists available at ScienceDirect

Sensors and Actuators B: Chemical

journal homepage: www.elsevier.com/locate/snb

Highly fluorescent probe for copper (II) ion based on commercially available compounds and live cell imaging

Duraisamy Udhayakumari [a], Sivan Velmathi [a,*], Yi-Ming Sung [b], Shu-Pao Wu [b]

[a] Organic and Polymer Synthesis Laboratory, Department of Chemistry, National Institute of Technology, Tiruchirappalli 620 015, India
[b] Department of Applied Chemistry, National Chiao Tung University, Hsinchu, Taiwan 300, Republic of China

ARTICLE INFO

Article history:
Received 27 December 2013
Received in revised form 11 March 2014
Accepted 16 March 2014
Available online 27 March 2014

Keywords:
Selectivity
Copper ion
Aqueous solution
Paramagnetic effect
PET
Bioimaging

ABSTRACT

The commercially available 2, 3-diaminophenazine, 1, 2-diamino-anthraquinone and 2, 4-dinitrophenylhydrazine (S**1**–S**3**) act as a colorimetric, fluorescent probes for selective detection of Cu^{2+} ions in aqueous medium over other metal ions. In presence of Cu^{2+}, S**1** shows fluorescent turn-off by the paramagnetic effect. S**2** and S**3** with Cu^{2+} ions show fluorescent turn-on due to the inhibition of photoinduced electron transfer mechanism. The fluorescent probes S**1**–S**3** detect Cu^{2+} ions in aqueous solution at nanomolar levels. Theoretical calculations were employed to understand the sensing mechanism of the sensors towards Cu^{2+}. S**1**, S**2** and S**3** were further applied for biological imaging to confirm that it can be used as a fluorescent probe for monitoring Cu^{2+} in living cells, and demonstrated its value in practical applications such as environmental and biological systems.

© 2014 Elsevier B.V. All rights reserved.

1. Introduction

The detection of metal ions is very important for analytical, environmental and biomedical applications due to their deleterious effects on human health and ecosystems [1–3]. Ion exchange chromatography, biochemical, electrochemical techniques and spectroscopic methods are used for the detection of metal ions, but those methods are quite difficult, higher in cost and unsuitable for on-line or field monitoring. Fluorescent sensors have more advantage such as simplicity, high sensitivity and selectivity. Therefore the fluorescence sensing of simple molecules has gained much attention in the field of environmental, medicine and biological chemistry [4–7]. Some of the metals play important role in living system, electrical and electronic industry. Copper plays a critical role as a catalytic cofactor for a variety of metalloenzymes, including superoxide dismutase, cytochrome c oxidase, tyrosinase and nuclease. Copper is one of the toxic metals [8–10], irregular ingestion of copper could cause lethargy and increased blood pressure [11–15]. The high level of copper causes neurodegenerative diseases such as Alzheimer's, Parkinson's and is also suspected to cause amyloidal precipitation and toxicity [16–23]. Various analytical methods and number of fluorescent probes have been developed for the detection of copper ions selectively as well as sensitively. But, only a few chemosensors in which the binding of a Cu^{2+} ion causes an increase in the fluorescence, have been reported [24–28]. However, the development of fluorescent sensor for copper ions in aqueous medium is an important task. In recent years, the design and syntheses of selective colorimetric and fluorescent copper probes have received great attention. The above mentioned probes are prepared by using certain organic synthesis process (single or multi step). But commercially available compounds have the advantages of cost effectiveness, simplicity, no need of organic synthesis process and field work applicability. Recently Lijun Qu et al., have reported a commercially available 1, 8-diamino naphthalene based fluorescence chemosensor for copper ions [29].

Herein, we report commercially available aromatic amines 1, 2-diaminophenazine, 1, 2-diamino-anthraquinone and 2, 4-dinitrophenylhydrazine (S**1**–S**3**) which detect copper ions selectively under four different channels (colorimetric, absorption, emission and bioimaging) in presence of other metal ions. Using these commercial available compounds as a starting material, many organic compounds are synthesized and reported mainly for anion sensing [30–35]. First time we report the commercially available 1, 2-diaminophenazine, 1, 2-diamino-anthraquinone and 2, 4-dinitrophenylhydrazine (S**1**–S**3**) as selective copper ion sensors. The fluorescent probes S**1**–S**3** detect Cu^{2+} ions in aqueous solution even at nanomolar levels. As the detection limit of S**2** and S**3** is

* Corresponding author. Tel.: +91 431 2503640/91 09486067404; fax: +91 431 2500133.
E-mail addresses: velmathis@nitt.edu, svelmathi@hotmail.com (S. Velmathi).

http://dx.doi.org/10.1016/j.snb.2014.03.063
0925-4005/© 2014 Elsevier B.V. All rights reserved.

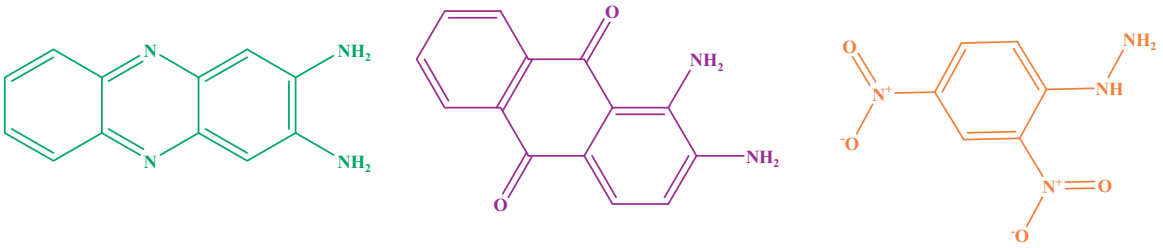

Fig. 1. Structure of sensors **1**, **2** and **3**.

0.15×10^{-9} M L^{-1}. These probes are highly sensitive. In case of S**1**, the quenching of the fluorescence emission is observed due to the paramagnetic nature of Cu^{2+} ions. But, enhancement of the fluorescence emission was observed in case of S**2** and S**3** bound with Cu^{2+}.

2. Materials and spectroscopic methods

2, 3-diaminophenazine, 1, 2-diamino-anthraquinone and 2, 4-dinitrophenylhydrazine, iron (III) chloride, cobalt (II) chloride, nickel (II) chloride, copper (II) chloride, zinc (II) acetate, cadmium (II) acetate, lead (II) acetate, mercury (II) nitrate, manganese (II) acetate, tin (II) chloride and chromium (III) chloride were purchased from Sigma–Aldrich and used as such. 5×10^{-5} M solution of S**1**–S**3** were prepared in acetonitrile (CH_3CN). 1.5×10^{-5} M solution of the cations was prepared in H_2O. To 3 ml of S**1** taken in the UV cuvette, 0.2 eq. (20 μL) – 2 eq. (200 μL) of Cu^{2+} solution was added. The same solutions were used for fluorescent titrations. ^1H and ^{13}C NMR were obtained on a Bruker 400 MHz spectrometer using $CDCl_3$ as solvent and tetramethylsilane (TMS) as an internal standard, IR spectrum was recorded by KBr pellet method on a Perkin–Elmer Spectrum One FTIR spectrometer. UV–visible spectra were recorded in UV-2600 a UV–vis spectrophotometer using 1 cm path length quartz cell. Fluorescence emission spectra were recorded in a Shimadzu RF-5301 PC spectrofluorophotometer at a scan rate of 500 nm/min. Excitation wavelength chosen was 300 nm for S**1** and S**3** and 400 nm for S**2**. Fluorescence imaging was performed with a Leica TCS-SP5-X AOBS Confocal microscope.

3. Results and discussion

3.1. Colorimetric sensing studies

Though the sensors S**1**–S**3** (Fig. 1) are well known and commercially available compounds. ^1H NMR spectroscopic studies (see supporting information) were done to check for the purity of the compounds.

The selective detection of environmentally active metal ions is investigated by visual, optical, fluorescence spectroscopy and bioimaging method. The sensors S**1**–S**3** were prepared in 5×10^{-5} M concentration in CH_3CN and all cations were prepared in 1.5×10^{-5} M concentration in H_2O. Sensors S**1**–S**3** were treated with various metal ions like Fe^{3+}, Co^{2+}, Ni^{2+}, Cu^{2+}, Zn^{2+}, Cd^{2+}, Pb^{2+}, Hg^{2+}, Mn^{2+}, Sn^{2+} and Cr^{3+} to study the sensitivity and selectivity towards particular metal ions over other metal ions. For the addition of 100 μL of all metal cations into S**1**–S**3**, the presence of Cu^{2+} ions shows colorimetric turn-off response from green to colorless for S**1** (Fig. 2a) and S**3** (Fig. 2c) and pink to colorless for S**2**

Fig. 2. a. Color changes of sensor **1** (5×10^{-5} M solution in CH_3CN) before and after the addition of 100 μL of respective cations (1.5×10^{-3} M solution in H_2O). b. Color changes of sensor **2** (5×10^{-5} M solution in CH_3CN) before and after the addition of 100 μL of respective cations (1.5×10^{-3} M solution in H_2O). c. Color changes of sensor **3** (5×10^{-5} M solution in CH_3CN) before and after the addition of 100 μL of respective cations (1.5×10^{-3} M solution in H_2O) (From the left to right: R, R + Fe^{3+}, R + Co^{2+}, R + Ni^{2+}, R + Cu^{2+}, R + Zn^{2+}, R + Cd^{2+}, R + Pb^{2+}, R + Hg^{2+}, R + Mn^{2+}, R + Sn^{2+} and R + Cr^{3+}).

(Fig. 2b), which could be easily distinguished by 'naked-eye'. The other cations like Fe^{3+}, Co^{2+}, Ni^{2+}, Zn^{2+}, Cd^{2+}, Pb^{2+}, Hg^{2+}, Mn^{2+}, Sn^{2+} and Cr^{3+} with S**1**–S**3** did not show any color change. Therefore Cu^{2+} could be easily identified among all other cations.

To know the interference of other metal ions in the Cu^{2+} ion detection of S**1**–S**3**, the competitive experiments were performed. Two equivalents of all the metal ions were added to the Cu^{2+} ion complex of S**1**–**S3** solution, but no changes were observed in the color of the S**1**–Cu^{2+}, S**2**–Cu^{2+} and S**3**–Cu^{2+} complex. This result is an added evidence for the high stability of the Cu^{2+} ion sensing, even in presence of other cations without any interference (see supporting information).

3.2. UV–vis spectroscopic studies

The binding ability of sensors (S**1**–S**3**) was further studied by optical spectroscopy. The UV–vis spectra of S**1**, S**2** and S**3** show strong absorption bands at 400 nm, 500 nm and 375 nm respectively. Fig. 3a–c shows the absorption spectrum of S**1**–S**3** with metal ions in aqueous medium. With the addition of Cu^{2+} into sensors (S**1**–S**3**), the intensities of the bands 400 nm (S**1**), 500 nm (S**2**) and 375 nm (S**3**) have been reduced. The other metal ions like Fe^{3+}, Co^{2+}, Ni^{2+}, Zn^{2+}, Cd^{2+}, Pb^{2+}, Hg^{2+}, Mn^{2+}, Sn^{2+} and Cr^{3+} ions did not show any optical changes with sensors S**1**–S**3**. From this, it is clear that S**1**–S**3** can detect Cu^{2+} selectively in presence of other metal ions. The incremental addition of Cu^{2+} ions into sensors (S**1**–S**3**), the corresponding absorption bands are gradually decreased (see supporting information) with isosbestic point at 425 nm for S**2**, 315 nm for S**3**. The relative absorbance of sensors (S**1**–S**3**) with all metal ions shows the selectivity of Cu^{2+} ions over other metal ions (see supporting information). Interestingly, the solution turned to colorless. The interaction and interference of Cu^{2+} ions with S**1**–S**3** were studied. Cu^{2+} was selectively sense in the presence of other metal ions. We have titrated S**1**–S**3** with 2 eq Cu^{2+} in presence of other metal ions like Fe^{3+}, Co^{2+}, Ni^{2+}, Zn^{2+}, Cd^{2+}, Pb^{2+}, Hg^{2+}, Mn^{2+}, Sn^{2+} and Cr^{3+}. There were no changes in the absorbance spectrum of S**1**/S**2**/S**3**–Cu^{2+} complex observed (see supporting information).

3.3. Fluorescence spectroscopic studies

Selectivity is a very important factor to estimate the performance of a new fluorescent probe. Highly selective detection of Cu^{2+} ions over other potentially competing species is a necessity. The fluorescence spectra of S**1**–S**3** change significantly along with the increased concentration of Cu^{2+} ions. Therefore, the selective response of S**1**–S**3** towards Cu^{2+} ions was studied in presence of various metal ions such as Fe^{3+}, Co^{2+}, Ni^{2+}, Zn^{2+}, Cd^{2+}, Pb^{2+}, Hg^{2+}, Mn^{2+}, Sn^{2+} and Cr^{3+}. The excitation wavelength selected for S**1** and S**3** is 300 nm and for S**2** is 400 nm. As shown in Fig. 4a, a clear fluorescence quenching is observed upon the addition of 100 μL of Cu^{2+} ions into S**1**. But the interaction of other mentioned ions with S**1** showed very little fluorescence intensity changes. The intensity of fluorescence band at 500 nm for S**1** ($\Phi = 0.51$) decreased gradually during the incremental addition of Cu^{2+} ions ($\Phi = 0.0033$) (see supporting information). Fluorescence quenching is measured quantitatively with Stern–Volmer equation. The calculated Stern–Volmer constant K_{sv} (M^{-1}) of sensor **1** with Cu^{2+} is 8.0×10^7 and linear regression correlation coefficient is 0.963, which suggests a linear correlation. The linearity in Stern–Volmer plots are interpreted in terms of the sphere of action defined in the dynamic quenching model. The fluorescence of S**2** and S**3** is highly enhanced in the presence of Cu^{2+}. Fig. 4b and c show the distinct fluorescence enhancement for S**2**–S**3** in presence of 100 μL Cu^{2+} ions. But the presence of other metal ions induces no significant change in the emission spectrum. The insert figures of Fig. 4a–c show the color change photographs for Cu^{2+} and the other metal ions under illumination with a 365 nm UV lamp. The gradual addition of Cu^{2+} ions into S**2** ($\Phi = 0.035$), the fluorescence band at 440 nm shifted (red Shift) to 475 nm with high intensity ($\Phi = 0.9$) (see supporting information) and a clear isosbestic point at 580 nm. The result revealed the coordination of Cu^{2+} ions with the amine (S**2**). A fluorescence titration experiment of S**3** ($\Phi = 0.15$) with Cu^{2+} ions was carried out. A linear increase in the fluorescence

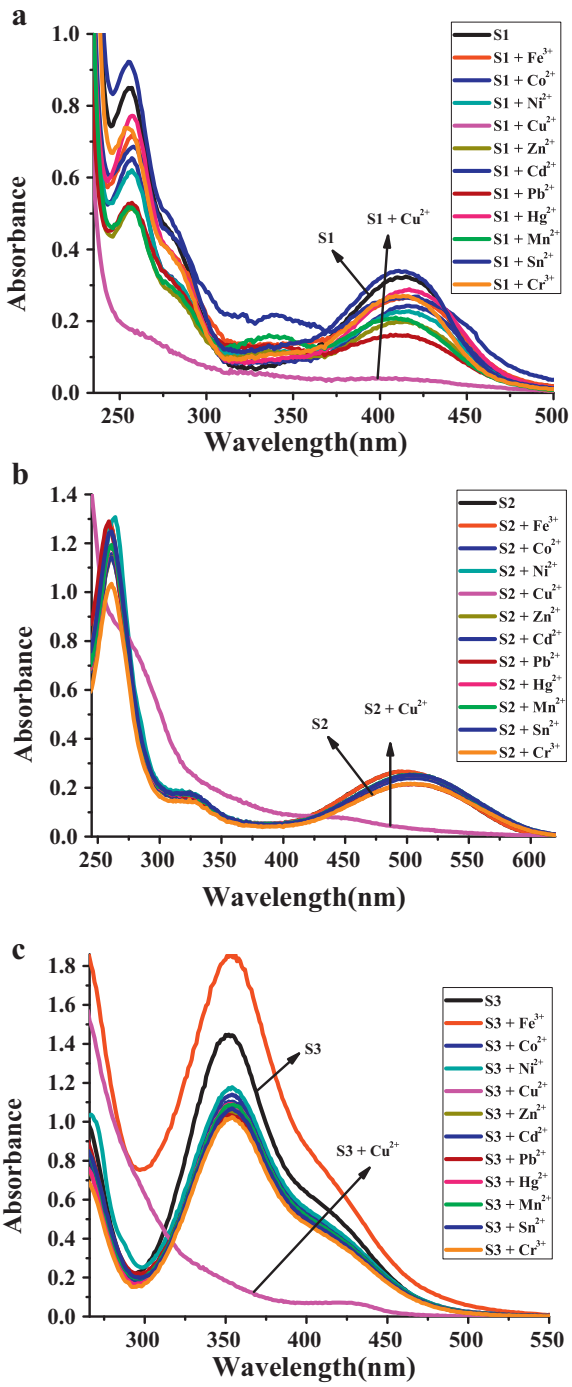

Fig. 3. a. UV–vis spectra of sensor **1** (5×10^{-5} M, in CH_3CN) upon titration with aqueous solution of cations (R, R + Fe^{3+}, R + Co^{2+}, R + Ni^{2+}, R + Cu^{2+}, R + Zn^{2+}, R + Cd^{2+}, R + Pb^{2+}, R + Hg^{2+}, R + Mn^{2+}, R + Sn^{2+} and R + Cr^{3+}). b. UV–vis spectra of sensor **2** (5×10^{-5} M, in CH_3CN) upon titration with aqueous solution of cations (R, R + Fe^{3+}, R + Co^{2+}, R + Ni^{2+}, R + Cu^{2+}, R + Zn^{2+}, R + Cd^{2+}, R + Pb^{2+}, R + Hg^{2+}, R + Mn^{2+}, R + Sn^{2+} and R + Cr^{3+}). c. UV–vis spectra of sensor **3** (5×10^{-5} M, in CH_3CN) upon titration with aqueous solution of cations (R, R + Fe^{3+}, R + Co^{2+}, R + Ni^{2+}, R + Cu^{2+}, R + Zn^{2+}, R + Cd^{2+}, R + Pb^{2+}, R + Hg^{2+}, R + Mn^{2+}, R + Sn^{2+} and R + Cr^{3+}).

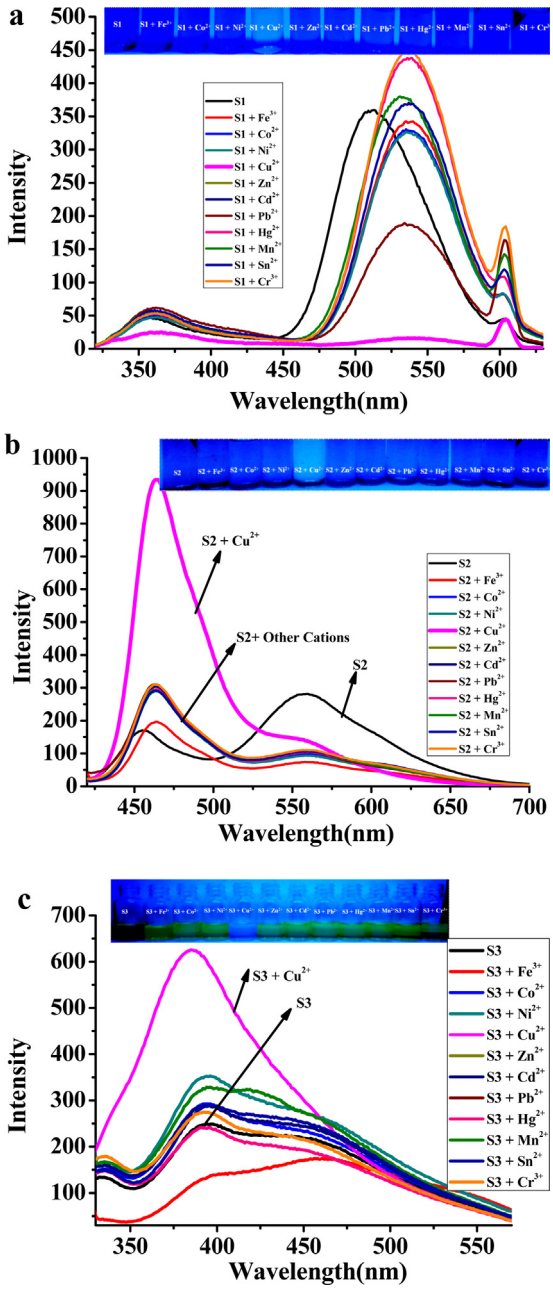

Fig. 4. a. Fluorescence spectra of sensor **1** (5×10^{-5} M, in CH_3CN) upon titration with aqueous solution of cations. b. Fluorescence spectra of sensor **2** (5×10^{-5} M, in CH_3CN) upon titration with aqueous solution of cations. (inset 4a and 4b): a color change photograph for Cu^{2+} and the other metal ions under illumination with a 365 nm UV lamp). c. Fluorescence spectra of sensor **3** (5×10^{-5} M, in CH_3CN) upon titration with aqueous solution of cations. (inset: a color change photograph for Cu^{2+} and the other metal ions under illumination with a 365 nm UV lamp).

intensity was observed with the increasing concentration of Cu^{2+} ions ($\Phi = 0.8$). Fig. 4d–f shows the relative fluorescence of S**1**–S**3** with all metal ions. The colorimetric responses of the S**1**–S**3** to other copper salts like Cu $(AcO)_2$, $CuCl_2$, $Cu(SO_4)_2$, $Cu(ClO_4)_2$ and $Cu(NO_3)_2$ was carried out (see supporting information). There is no divergence in fluorescence intensity in the presence of other copper salts. From this result it can be inferred that Cu^{2+} ions selectively sense in the presence of counter anions (see supporting information).

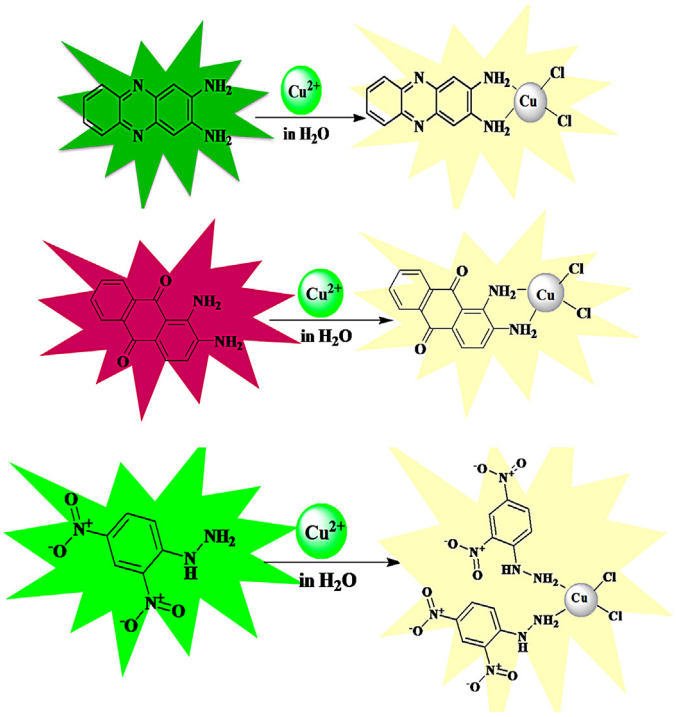

Fig. 5. Binding mode of Sensor **1**–**3** with Cu^{2+} ion.

3.4. Binding constant, detection limit and jobs plot studies

Benesi–Hildebrand method has become one of the most common strategies for determining association constants based on the absorbance spectra. Using Benesie Hildebrand expression, the binding constants of S**1**–S**3** with Cu^{2+} were investigated. The corresponding measured absorbance $[1/(A - A_0)]$ for S**1**–S**3** has varied as a function of $1/[Cu^{2+}]$ in a non-linear relationship. The binding constants of S**1**–S**3** with Cu^{2+} are 3.3×10^5, 3.3×10^5 and 2.8×10^5 respectively. Job's plot studies indicate host–guest molecular complexation, the sensors S**1**and S**2** with Cu^{2+} ions form 1:1 stoichiometry whereas S**3** with Cu^{2+} ions form 2:1 stoichiometry (Fig. 5) (see supporting information). Using fluorescence titration experiments of S**1**–S**3** with Cu^{2+} ions, the detection limits were calculated. The detection limit was then calculated with the equation: detection limit = $3\sigma_{bi}/m$, where σ_{bi} is the standard deviation of blank measurements and m is the slope of the intensity versus sample concentration. The detection limits of Cu^{2+} ion with S**1**–S**3** are 0.23 sub-nM, 0.15 nM, 0.15 nM respectively. The stoichiometries of the complexes discussed above coincide with the previous reports [29,36]. The detection limit, interference with other metals of S1, S2 and S3 was compared with the previously reported probes (Table 1) [37–40].

3.5. Effect of pH

The influence of pH on S**1**–S**3** was studied using fluorescence spectroscopic method (see supporting information). In S**1** over a pH range of 4–8, the fluorescence quenching band at 520 nm was unchanged. When the pH value exceeded 8, the intensity at 520 nm increased. This was due to the dissociation of S**1**–Cu^{2+} complexes. At pH values less than 4, absorbance was almost negligible; evidently the S**1**–Cu^{2+} complexes do not exist over this pH range. For sensor **2**–Cu^{2+} complexes, the intensity at the wavelength 500 nm suddenly increased at pH 5.0 and reached maximum at pH 8.0. This indicates that the formation of S**2**–Cu^{2+} complexes is a deprotonation process. When the pH value exceeded 8.0, the intensity

Table 1
Comparison of S1, S2 and S3 with the previously reported probes.

Sensors	Detection limit	Interference	Sensing metals	Reference
2,3-diaminophenazine based sensor	2.24 nM	None	Hg^{2+}	[37]
2,3-diaminophenazine based sensor	1 nM	None	Hg^{2+}	[38]
Commercial 2,3-diaminophenazine	0.23 sub-nM	None	Cu^{2+}	Our work
1, 2-Diamino-anthraquinone based sensor	None	None	Zn^{2+}	[39]
Commercial 1,2-diamino-anthraquinone	0.15 nM	None	Cu^{2+}	Our work
2,4-dinitrophenylhydrazine based sensor	None	None	Ca^{2+}	[40]
Commercial 2,4-dinitrophenylhydrazine	0.15 nM	None	Cu^{2+}	Our work

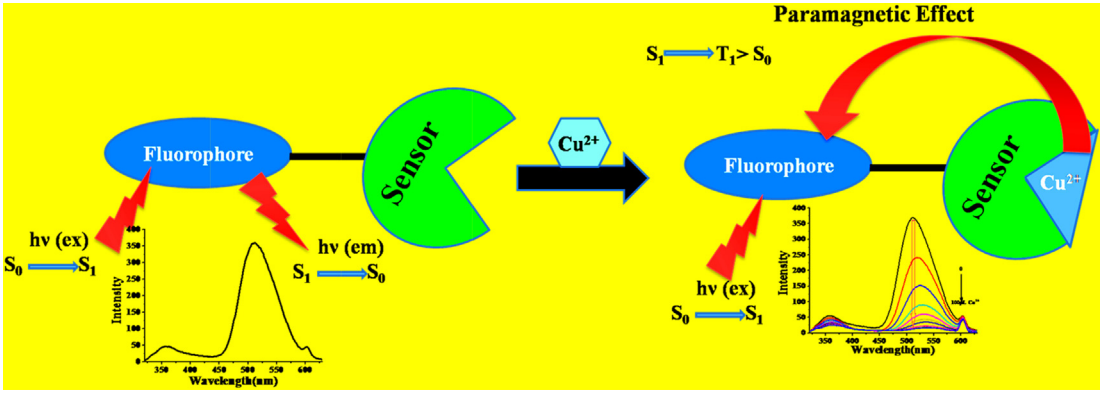

Fig. 6. Paramagnetic fluorescence quenching of S**1**.

at 475 nm gradually decreased, due to the dissociation of S**2**–Cu^{2+} complexes. The effect of pH on the formation of S**3**–Cu^{2+} complexes was also studied. For the S**3**–Cu^{2+} complexes, the emission at the wavelength 380 nm increased sharply at pH 5.0 and no intensity changes up to pH 9.5. This also indicates that the formation of S**3**–Cu^{2+} complexes is a deprotonation process.

3.6. Sensing mechanism

The coordination of metal ions could cause an enhancement of the fluorescence or quenching of the fluorescence intensity. The enhancement of fluorescence emission is called Chelation Enhanced Fluorescence effect (CHEF). The quenching of the fluorescence is called Chelation Enhancement Quenching effect (CHEQ). Both effects can be coupled with a red or blue shift of the emission band. S**1** with Cu^{2+} shows the fluorescence quenching; via paramagnetic fluorescence quenching. In a wide variety of metal complexes, the forbidden intersystem crossing (isc) becomes faster due to the presence of a d^9 Cu (II) ion paramagnetic atom in the proximity of the fluorophore. These complexes undergo inter system crossing by excitation, from S**1** to T**1** state of the fluorophore that can be deactivated by bimolecular non-radiative processes (Fig. 6). In case of S**2** and S**3**, binding with Cu^{2+} ions, fluorescence enhancement occurred due to the Photoinduced Electron Transfer (PET) mechanism. S**2** and S**3** show weak fluorescence, PET takes place from the lone pair (N) of the coordinating atoms to the HOMO of the excited fluorophore. The presence of a Cu^{2+} ion lowers the energy of the lone pair involved in the coordination preventing the PET, thus causing the switch-ON mechanism of the fluorescence (Fig. 7).

3.7. Theoretical calculation study

Density Functional Theory (DFT) calculations have been used to understand the behaviour of S**1**–S**3** with the Cu^{2+} ions. Highest occupied molecular orbital (HOMO) and lowest unoccupied molecular orbital (LUMO) for S**1**–S**3** and their metal complexes have been generated from optimized structures of the sensors S**1**–S**3** and their respective metal complexes (Fig. 8). The structural optimization and the computational calculations were carried out using Gaussian09 quantum chemistry package and results were viewed with GaussView5 GUI. The appropriate choice of model chemistry for the computation of electronic structure property is indispensable. In the present scenario, Density Functional Theory (DFT) supported B3LYP/6-31G (d, p) model chemistry was implemented particularly for Schiff base ligands under gas phase condition. But its metal complexes were modeled using effective core potential (ECP) based LANL2DZ (Los Alamos National Laboratory 2-double-z–Acronyms)

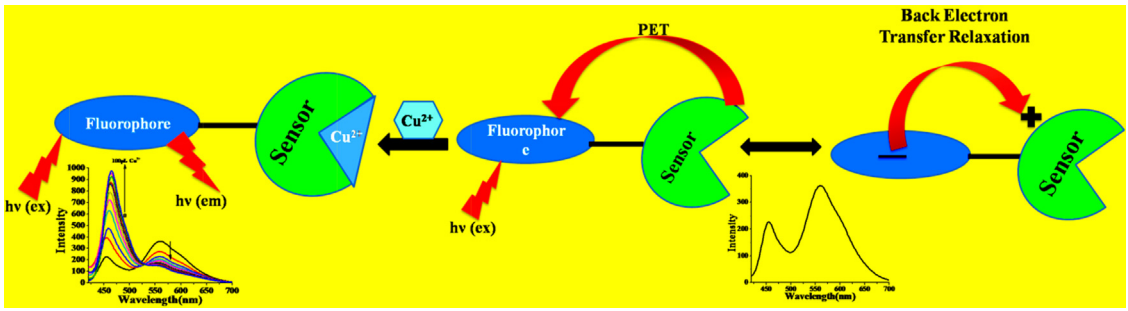

Fig. 7. Photoinduced electron transfer (PET) mechanism of S**2** and S**3**.

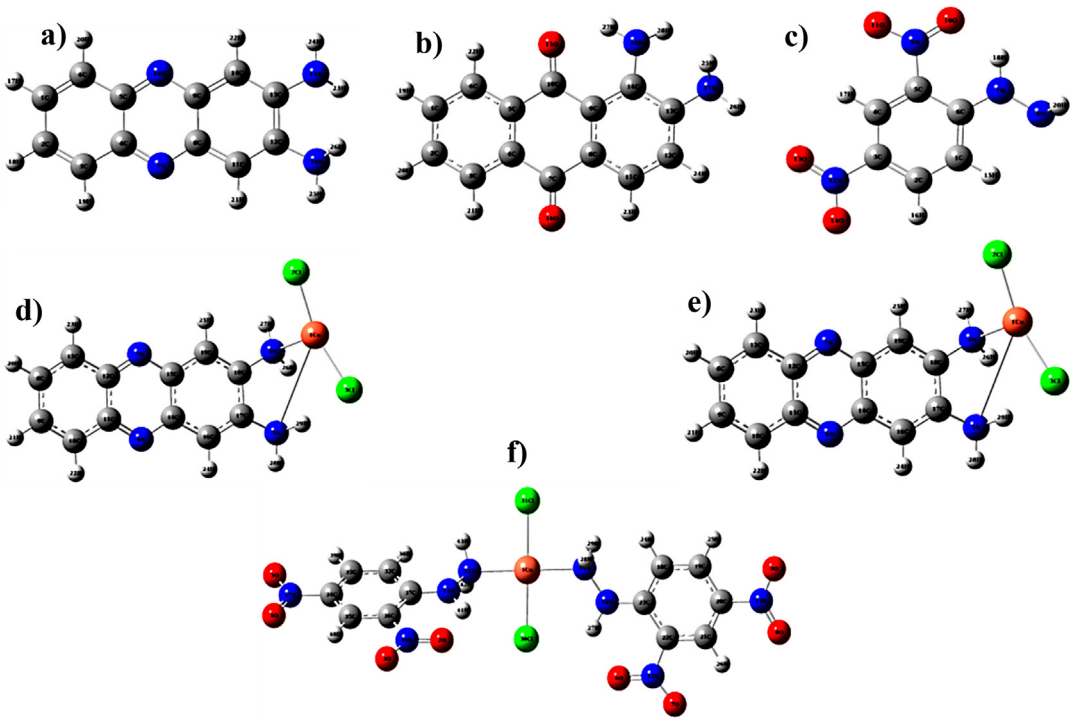

Fig. 8. Optimized structures of (a) S**1**, (b) S**2**, (c) S**3,** (d) S**1** + Cu (II) (e) S**2** + Cu (II) and (f) S**3** + Cu (II).

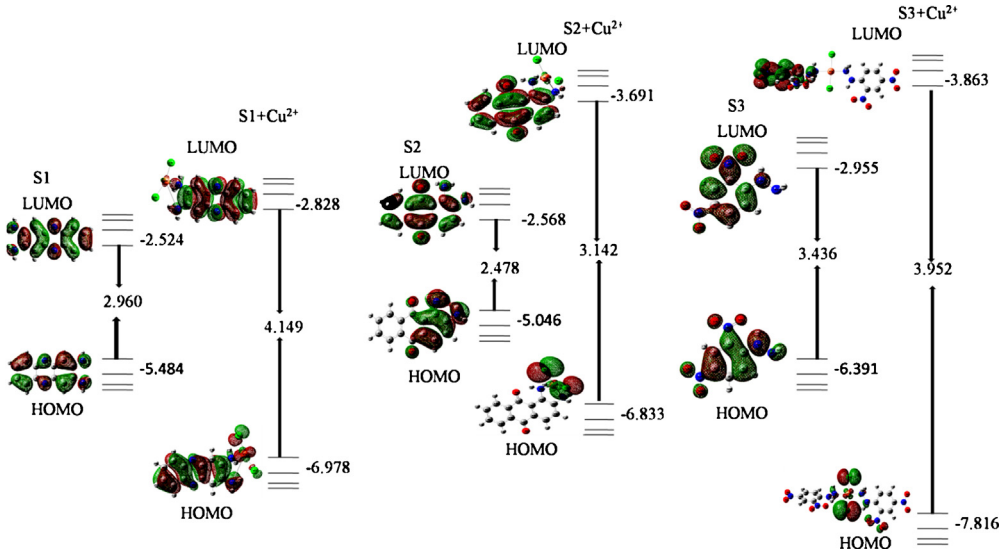

Fig. 9. Energy levels of various HOMO and LUMO's of S**1**–S**3** in the absence and presence of Cu (II).

basis set to optimize the geometry of the complex. The metal atom present in the complex was treated under LANL2DZ where as other atoms are manipulated with B3LYP/6-31G (d, p) level of theory. DFT calculations were carried out to investigate the change of the absorption spectra upon the addition of Cu^{2+}. From the energy level diagram (Fig. 9), it can be seen that the addition of the metal ions lead to the stabilization of the HOMO and LUMO of the sensor molecule. From the calculated results, the energy levels of HOMO

Table 2
Energies of HOMO and LUMO of the S**1**–S**3** and complexes.

Ligands & metal complexes	HOMO (eV)	LUMO (eV)	ΔE (eV)	Theoretical wavelength (nm)	Observed wavelength (nm)
S**1**	−5.484	−2.524	2.960	405 nm	414 nm
S**1** + Cu(II)	−6.978	−2.828	4.149	292 nm	308 nm
S**2**	−5.046	−2.568	2.478	484 nm	499 nm
S**2** + Cu(II)	−6.833	−3.691	3.142	382 nm	373 nm
S**3**	−6.391	−2.955	3.436	349 nm	352 nm
S**3** + Cu(II)	−7.816	−3.863	3.952	343 nm	299 nm

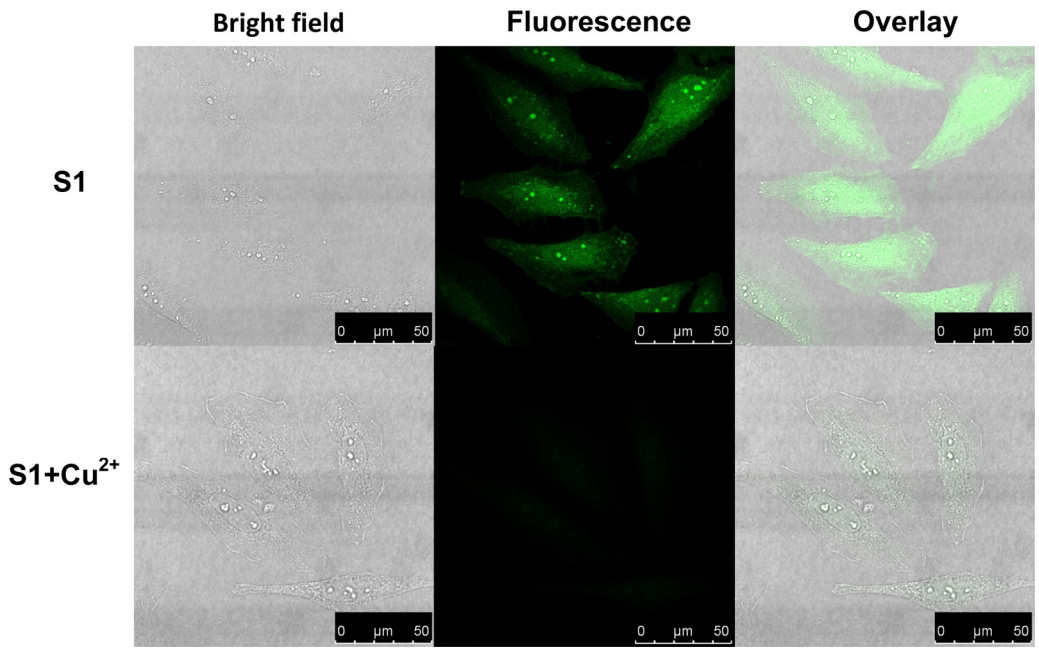

Fig. 10. Fluorescence images of HeLa cells treated with **S1** and Cu^{2+}. Bright field image (left), fluorescence image (middle) and merged image (right). The scale bar is 50 μm.

and LUMO of S**1**–S**3** increased after the addition of Cu^{2+} ions when compared to that of the free S**1**–S**3** (Table 2). For Cu^{2+} complexes of S**1**–S**3**, the absorption peaks predicted by the theoretical methods is blue-shifted compared with those of the independent probes, which is in good agreement with the experimental observations.

3.8. Cell imaging study

To determine the applicability of S**1**–S**3** for practical applications, bio imaging studies in living cells were done. HeLa cells were grown in H-DMEM (Dulbecco's Modified Eagle's Medium, high glucose) supplemented with 10% FBS (Fetal Bovine Serum) in an atmosphere of 5% CO_2 at 37 °C. The cells cultured in DMEM were treated with 10 mM solutions of Cu^{2+} (2 μL; final concentration: 20 μM) dissolved in sterilized PBS (Phoshphate Buffered Saline) (pH 7.4) and incubated at 37 °C for 30 min. The treated cells were washed with PBS (2 mL × 3) to remove remaining metal ions. DMEM (2 mL) was added to the cell culture, which was then treated with a 10 mM solution of chemosensor S**1** (2 μL; final concentration: 20 μM) dissolved in DMSO. The samples were incubated at 37 °C for 30 min. The culture medium was removed, and the treated cells were washed with PBS (2 mL × 3) before observation. For S**1**,

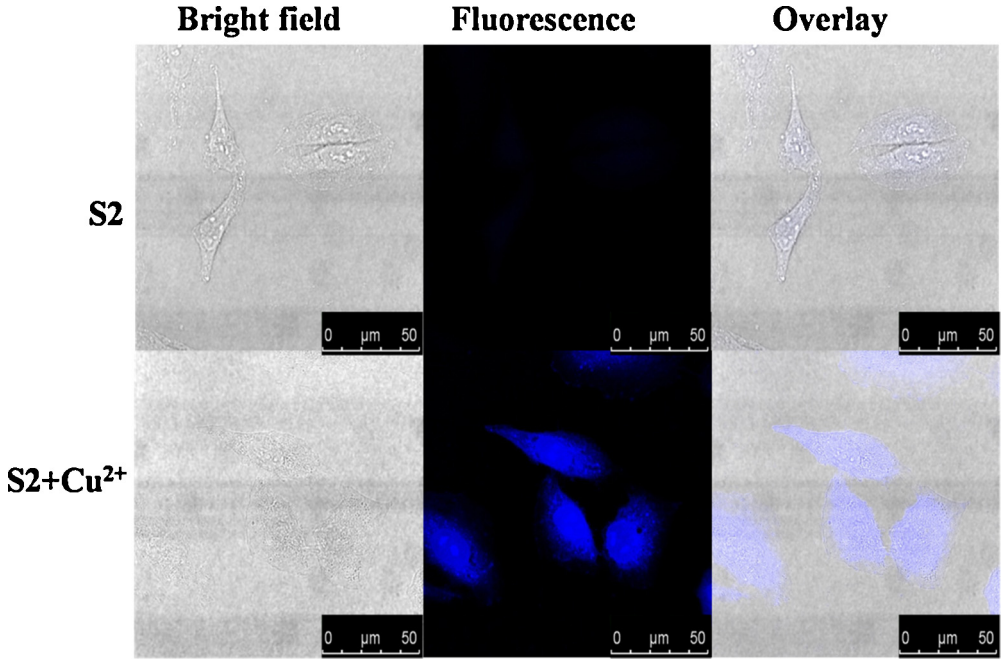

Fig. 11. Fluorescence images of HeLa cells treated with **S2** probe and Cu^{2+}. Bright field image (left), fluorescence image (middle) and merged image (right). The scale bar is 25 μm.

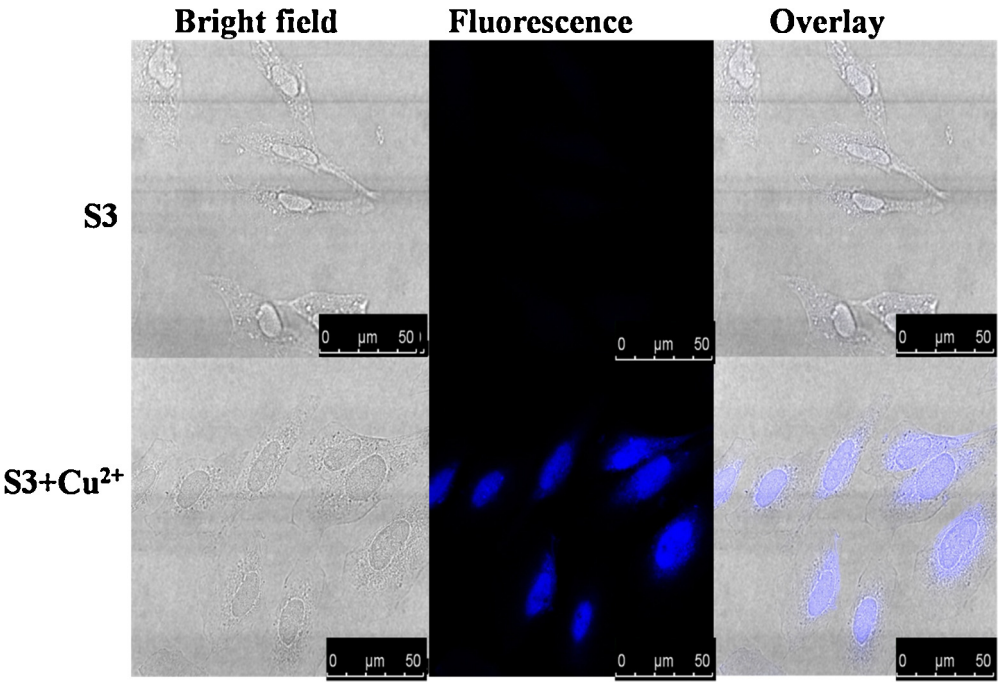

Fig. 12. Fluorescence images of HeLa cells treated with **S3** probe and Cu^{2+}. Bright field image (left), fluorescence image (middle) and merged image (right). The scale bar is 25 μm.

the cells were excited with a white light laser at 405 nm, and emission was collected at 510 Â ± 25 nm for S**1** and at 463 Â ± 25 nm for S**2** and S**3**. From this study, the green fluorescence was observed from cells *HeLa* cells stained with S**1** and copper ions (Fig. 10) whereas blue fluorescence was observed from *HeLa* cells stained with S**2** (Fig. 11), S**3** (Fig. 12) and copper ions. The significant green and blue fluorescence from the intracellular region proves that S**1**–S**3** are applicable for imaging Cu^{2+} in living cells. The bioimaging in the *HeLa* cells confirm the fluorescence quenching and fluorescence enhancement with excellent cell permeability. It shows that S**1**–S**3** are biocompatible in nature and can be used for detecting Cu^{2+} ions in cell rapidly.

4. Conclusion

In conclusion, we have brought out the potential of commercially available compounds (S**1**–S**3**), for the selective detection of Cu^{2+} ions over the other interfering metal ions. The sensors (S**1**–S**3**) showed specific selectivity for Cu^{2+} ions in aqueous medium. Investigation of the recognition mechanism indicates that S**1** and S**2** recognize Cu^{2+} by forming a stable 1:1 complex whereas S**3** forms a stable 2:1 S**3**–Cu^{2+} complex. The detection limits of S**1**–S**3** towards Cu^{2+} ions were 0.23 sub-nM (S**1**), 0.15 nM (S**2**) and 0.15 nM (S**3**) respectively, which indicate that the sensors S**1**–S**3** are the potential colorimetric sensors for monitoring Cu^{2+} ions in physiological and environmental systems. The fluorescence properties of sensors in the presence of Cu^{2+} ions were evaluated. The significant fluorescence quenching was probably caused by S**1** coordinated with Cu^{2+}, the paramagnetic effect from spin-orbit coupling of the Cu^{2+}. On the other hand, the fluorescence of S**2** and S**3** was remarkably enhanced upon addition of Cu^{2+}. This enhancement may be due to the inhibition of photoinduced electron transfer mechanism (PET). The value of these sensor systems (S**1**–S**3**) has been demonstrated by its use in detecting Cu^{2+} ions in living cells.

Acknowledgment

Authors express their thanks to DRDO (ERIP/ER/1006004/M/01/1333 dated 23-05-2011) for financial assistance in the form of a major sponsored project.

Appendix A. Supplementary data

Supplementary data associated with this article can be found, in the online version, at http://dx.doi.org/10.1016/j.snb.2014.03.063.

References

[1] V. Dujols, F. Ford, A.W. Czarnik, A long-wavelength fluorescent chemodosimeter selective for Cu (II) ion in water, J. Am. Chem. Soc. 119 (1997) 7386–7387.
[2] M. Angelova, S. Asenova, V. Nedkova, R. Koleva-Kolarova, Copper in the human organism, Trakia. J. Sci. 9 (2011) 88–98.
[3] R. Uauy, M. Olivares, M. Gonzalez, Essentiality of copper in humans, Am. J. Clin. Nutr. 67 (1998) 952–959.
[4] T. Mori, K. Akamatsu, M. Okamoto, M. Sumita, Y. Tateyama, H. Sakai, J.P. Hill, M. Asahiko Abe, K. Ariga, Micrometer-level naked-eye detection of caesium particulates in the solid state, Sci. Technol. Adv. Mater. 14 (2013) 015002.
[5] Y. Yang, Q. Zhao, W. Feng, F. Li, Luminescent chemodosimeters for bioimaging, Chem. Rev. 113 (2013) 192–270.
[6] K. Ariga, H. Ito, J.P. Hilla, H. Tsukube, Molecular recognition: from solution science to nano/materials technology, Chem. Soc. Rev. 41 (2012) 5800–5835.
[7] S.J. Butler, D. Parker, Anion binding in water at lanthanide centres: from structure and selectivity to signalling and sensing, Chem. Soc. Rev. 42 (2013) 1652–1666.
[8] H. Tapiero, D.M. Townsend, K.D. Tew, Trace elements in human physiology and pathology. Copper, Biomed. Pharmacother. 57 (2003) 386–398.
[9] R. Uauy, M. Olivares, M. Gonzalez, Essentiality of copper in humans, Biomed. Pharmacother. 57 (2003) 134–144.
[10] J. Huller, M.T. Pham, S. Howitz, Thin layer copper ISE for fluidicmicro system, Sensor. Actuat. B 91 (2003) 17–20.
[11] A.W. Varnes, R.B. Dodson, E.L. Wehry, Interactions of transition-metal ions with photoexcited states of flavines. Fluorescence quenching studies, J. Am. Chem. Soc. 94 (1972) 946–950.
[12] A. deSilva, H.Q. Nimal Gunaratne, T. Gunnlaugsson, A.J.M. Huxley, C.P. McCoy, J.T. Rademacher, T.E. Rice, Signaling recognition events with fluorescent sensors and switches, Chem. Rev. 97 (1997) 1515–1566.

[13] Y. Zheng, J. Orbulescu, X. Ji, F.M. Andreopoulos, S.M. Pham, R.M. Leblanc, Development of fluorescent film sensors for the detection of divalent copper, J. Am. Chem. Soc. 125 (2003) 2680–2686.
[14] V.A. Rapisarda, S.I. Volentini, R.N. Farias, E.M. Massa, Quenching of batho cuproine disulfonate fluorescence by Cu(I) as a basis for copper quantification, Anal. Biochem. 307 (2002) 105–109.
[15] H.S. Jung, P.S. Kwon, J.W. Lee, J. Kim, C.S. Hong, J.W. Kim, S. Yan, J.Y. Lee, J.W. Lee, T. Joo, S. Kim, Coumarin derived Cu^{2+} selective fluorescence sensor: synthesis, mechanisms, and applications in living cells, J. Am. Chem. Soc. 131 (2009) 2008–2012.
[16] D.J. Waggoner, T.B. Bartnikas, J.D. Gitlin, The role of copper in neurodegenerative disease, Neurobiol. Dis. 6 (1999) 221–230.
[17] C. Vulpe, B. Levinson, S. Whitney, S. Packman, J. Gitschier, Isolation of a candidate gene for Menkes disease and evidence that it encodes a copper-transporting ATPase, Nat. Genet. 3 (1993) 7–13.
[18] P.C. Bull, G.R. Thomas, J.M. Rommens, J.R. Forbes, D.W. Cox, The Wilson disease gene is a putative copper transporting P-type ATPase similar to the Menkes gene, Nat. Genet. 5 (1993) 327–337.
[19] K.J. Barnham, C.L. Masters, A.I. Bush, Neurodegenerative diseases and oxidative stress, Nat. Rev. Drug Discov. 3 (2004) 205–214.
[20] J.S. Valentine, P.J. Hart, Misfolded CuZnSOD and amyotrophic lateral sclerosis, Proc. Natl. Acad. Sci. 100 (2003) 3617–3622.
[21] L.I. Bruijn, T.M. Miller, D.W. Cleveland, Unraveling the mechanisms involved in motor neuron degeneration in ALS, Annu. Rev. Neurosci. 27 (2004) 723–749.
[22] D.R. Brown, H. Kozlowski, Biological inorganic and bioinorganic chemistry of neurodegeneration based on prion and Alzheimer diseases, Dalton Trans. 13 (2004) 1907–1917.
[23] P.G. Georgopoulos, A. Roy, M.J. Yonone-Lioy, R.E. Opiekun, P.J. Lioy, Environmental copper: its dynamics and human exposure issues, J. Toxicol. Environ. Health Part B 4 (2001) 341–394.
[24] M.H. Mashhadizadeh, M.R. Zadmehr, H. Allah-Abadi, Selective preconcentraion and solid phase extraction of ultra trace copper(II) from natural water and human hair and determination by atomic absorption spectroscopy, Asian J. Chem. 18 (2006) 137–144.
[25] M.X. Yu, M. Shi, Z.G. Chen, F.Y. Li, X.X. Li, Y.H. Gao, J. Xu, H. Yang, Z.G. Zhou, T. Yi, C.H. Huang, Highly sensitive and fast responsive fluorescence turn-on chemodosimeter for Cu^{2+} and its application in live cell imaging, Chem. Eur. J. 14 (2008) 6892–6900.
[26] J. Huang, Y. Xu, X. Qian, A red-shift colorimetric and fluorescent sensor for Cu^{2+} in aqueous solution: unsymmetrical 4,5-diaminonaphthalimide with N–H deprotonation induced by metal ions, Org. Biomol. Chem. 7 (2009) 1299–1303.
[27] Y. Zhou, F. Wang, Y. Kim, S.J. Kim, J. Yoon, Cu^{2+} selective ratiometric and Off–On sensor based on the rhodamine derivative bearing pyrene group, Org. Lett. 11 (2009) 4442–4445.
[28] T. Gunnlaugsson, J.P. Leonard, N.S. Murray, Highly selective colorimetric naked-eye Cu(II) detection using an azobenzene chemosensor, Org. Lett. 6 (2004) 1557–1560.
[29] L. Qu, C. Yin, F. Huo, Y. Zhang, Y. Li, A commercially available fluorescence chemosensor for copper ion and its application in bioimaging, Sensor. Actuat. B 183 (2013) 636–640.
[30] S.M.S. Chauhan, T. Bisht, B. Garg, Anion sensing by phenazine-based urea/thiourea receptors, Tetrahedron Lett. 49 (2008) 6646–6649.
[31] R.M.F. Batista, E. Oliveira, S.P.G. Costa, C. Lodeiro, M.M.M. Raposo, Synthesis and ion sensing properties of new colorimetric and fluorimetric chemosensors based on bithienyl-imidazo-anthraquinone chromophores, Org. Lett. 9 (2007) 3201–3204.
[32] X. Peng, Y. Wu, J. Fan, M. Tian, K. Han, Colorimetric and ratiometric fluorescence sensing of fluoride: tuning selectivity in proton transfer, J. Org. Chem. 70 (2005) 10524–10531.
[33] D.A. Jose, D.K. Kumar, B. Ganguly, A. Das, Efficient and simple colorimetric fluoride ion sensor based on receptors having urea and thiourea binding sites, Org. Lett. 6 (2004) 3445–3448.
[34] D. Fan, B. Zhang, K. Deng, Colorimetric sensing of fluoride based on acenaphthenequinone 2, 4-dinitrophenylhydrazone, J. Mat. Sci. Eng. A 2 (2012) 712–716.
[35] A.K. Mahapatra, G. Hazra, J. Roy, P. Sahoo, A simple coumarin-based colorimetric and ratiometric chemosensor for acetate and a selective fluorescence turn-on probe for iodide, J. Lumin. 131 (2011) 1255–1259.
[36] Z. Chen, L. Wang, G. Zou, J. Tang, X. Cai, M. Teng, L. Chen, Highly selective fluorescence turn-on chemosensor based on naphthalimide derivatives for detection of copper(II) ions, Spectrochim. Acta A. 105 (2013) 57–61.
[37] L. Yan, Z. Chen, Z. Zhang, C. Qu, L. Chen, D. Shen, Fluorescent sensing of mercury(II) based on formation of catalytic gold nanoparticles, Analyst 138 (2013) 4280–4283.
[38] S. Liu, X. Qin, J. Tian, L. Wang, X. Sun, Photochemical preparation of fluorescent 2,3-diaminophenazine nanoparticles for sensitive and selective detection of Hg(II) ions, Sensor. Actuat. B 171-172 (171) (2012) 886–890.
[39] H.M. Chawla, R. Shukla, S. Pandey, Preferential recognition of zinc ions through a new anthraquinonoidal calix[4]arene, Tetrahedron Lett. 53 (2012) 2996–2999.
[40] N.Y. Kim, S.K. Chang, Calix[4]arenes bearing two distal azophenol moieties: highly selective chromogenic ionophores for the recognition of Ca^{2+} ion, J. Org. Chem. 63 (1998) 2362–2364.

Biographies

Ms. Duraisamy Udhayakumari was born in 1989. She received her Under Graduate degree from Vellalar College for Women, Erode in the year 2009 and Masters degree from National Institute of Technology, Trichy in the year 2011. Currently she is doing her PhD in the same institute under the guidance of Dr. S. Velmathi. Her research is focused on the synthesis of novel chromogenic and fluorogenic organic receptors for the recognition of anions/cations and their utilizations in the real samples.

Dr. Sivan Velmathi was born in 1974 in Chennai, India. She received her PhD degree in Organic Chemistry from the University of Madras in the year 2001. Currently, she is working as an Associate Professor in Department of Chemistry (Organic and Polymer Synthesis Laboratory), National Institute of Technology, Trichy. Her research interests focus on development of new materials and their application as sensors and homogenous and heterogeneous catalytic asymmetric synthesis. She has published around 65 papers in highly reputed journals and holds three patents.

Yi-Ming Sung is studying for PhD in the Department of Applied Chemistry at National Chiao Tung University.

Dr. Shu-Pao Wu had Ph.D. in 2004, Department of Chemistry, The Ohio State University, USA. Currently, he is working as an Associate Professor in Department of Applied Chemistry National Chiao Tung University, Taiwan, Republic of China. Current interests: metal ion chemosensors and AlkB.